Sensor Influence in the Performance of Simultaneous Mobile Robot Localization and Map Building*

J.A. Castellanos J.M.M. Montiel J. Neira J.D. Tardós

Departamento de Informática e Ingeniería de Sistemas
Universidad de Zaragoza, Spain
E-mail: {jacaste, josemari, jneira, tardos}@posta.unizar.es

Abstract: Mobile robot navigation in unknown environments requires the concurrent estimation of the mobile robot localization with respect to a base reference and the construction of a global map of the navigation area. In this paper we present a comparative study of the performance of the localization and map building processes using two distinct sensorial systems: a rotating 2D laser rangefinder, and a trinocular stereo vision system.

1. Introduction

Simultaneous localization and map building is one of the key problems in autonomous mobile robot navigation. Different approaches have been reported in the literature after the initial theoretical contributions of Smith et al. [1] and the early experiments of Chatila et al. [2] and Leonard et al. [3]. An important application in which we are interested is the development of the sensorial system for autonomous wheel-chairs for handicapped people. Information gathered by the sensorial system would be used for navigation purposes. Both the localization of the vehicle and the construction of a map of its surroundings are required. The main goal of this paper is to discuss the issues concerning the type of sensor used by the system. We present a comparative study of the performance of the localization and map building processes using two distinct sensorial systems: a 2D laser rangefinder, and a trinocular vision system.

In our approach we use a probabilistic model, the Symmetries and Perturbation Model (SPmodel) [4, 5], to represent uncertain geometric information given by any sensor in a general and systematic way. As reported in the literature, the solution to the simultaneous robot localization and map building problem requires maintaining a representation of the relationships between the location estimations of the robot and the features included in the map [6, 7], which in our work are represented by the cross-correlations between their estimations. In this paper we briefly present the formulation of the Symmetries and Perturbations Map (SPmap), a probabilistic framework for the simultaneous

*This work has been supported by spanish CICYT project TAP97-0992-C02-01

localization and map building problem whose main advantage is its generality, i.e. sensor and feature independence.

The rest of the paper is structured as follows. In section 2 we describe our approach to the simultaneous localization and map building problem. Section 3 presents the experiment performed and the sensor data processing algorithms used. Experimental results obtained with a 2D laser rangefinder and a trinocular vision system are discussed in section 4, whilst the main conclusions of our work are drawn in the last section.

2. Simultaneous Localization and Map Building

2.1. The Symmetries and Perturbation Model

In our feature-based approach, uncertain geometric information is represented using a probabilistic model: the Symmetries and Perturbation Model (SPmodel) [4, 5] which combines the use of probability theory to represent the imprecision in the location of a geometric element, and the theory of symmetries to represent the partiallity due to characteristics of each type of geometric element.

In the SPmodel, the location of a geometric element E with respect to a base reference W is given by a *location vector* $\mathbf{x}_{WE} = (x,\ y,\ \phi)^T$. The estimation of the location of an element is denoted by $\hat{\mathbf{x}}_{WE}$, and the estimation error is represented locally by a *differential location vector* $\mathbf{d}_E$ relative to the reference attached to the element. Thus, the true location of the element is:

$$\mathbf{x}_{WE} = \hat{\mathbf{x}}_{WE} \oplus \mathbf{d}_E \tag{1}$$

where $\oplus$ represents the composition of location vectors. To account for the symmetries of the geometric element, we assign in $\mathbf{d}_E$ a null value to the degrees of freedom corresponding to them, because they do not represent an effective location error. We call *perturbation vector* the vector $\mathbf{p}_E$ formed by the non null elements of $\mathbf{d}_E$. Both vectors can be related by a row selection matrix $\mathbf{B}_E$ that we call *self-binding matrix* of the geometric element:

$$\mathbf{d}_E = \mathbf{B}_E^T \mathbf{p}_E \quad ; \quad \mathbf{p}_E = \mathbf{B}_E \mathbf{d}_E \tag{2}$$

Then, the *uncertain location* of every geometric entity is represented in the SPmodel by a quadruple $\mathbf{L}_{WE} = (\hat{\mathbf{x}}_{WE}, \hat{\mathbf{p}}_E, \mathbf{C}_E, \mathbf{B}_E)$, where the transformation $\hat{\mathbf{x}}_{WE}$ is an estimation taken as base for perturbations, $\hat{\mathbf{p}}_E$ is the estimated value of the perturbation vector, and $\mathbf{C}_E$ its covariance.

2.2. The Symmetries and Perturbation Map

The Symmetries and Perturbation Map (SPmap) is a complete representation of the environment of the robot which includes the uncertain location of the mobile robot $\mathbf{L}_{WR}$, the uncertain locations of the features obtained from sensor observations $\mathbf{L}_{WF_i}, i \in \{1 \dots N_F\}$ and their interdependencies. The SPmap can be defined as a quadruple:

$$\mathbf{SPmap} = \left(\hat{\mathbf{x}}^W,\ \hat{\mathbf{p}}^W,\ \mathbf{C}^W,\ \mathbf{B}^W\right) \tag{3}$$

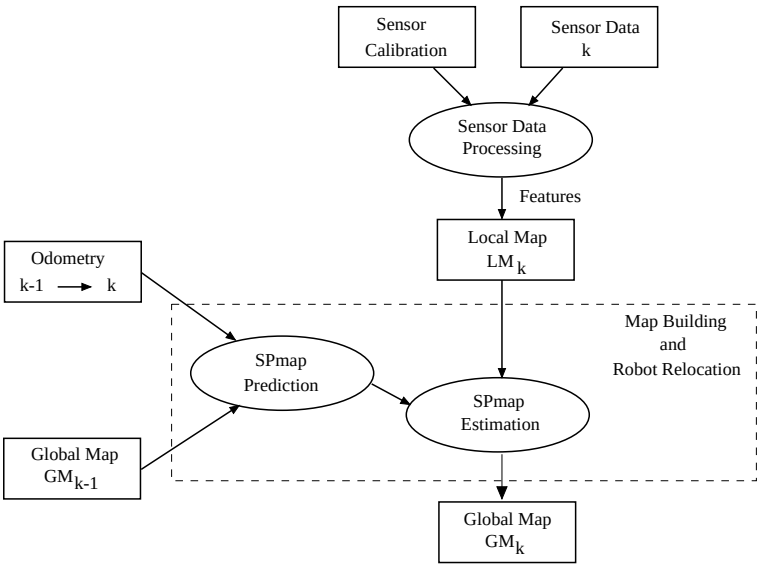

Figure 1. Simultaneous mobile robot localization and map building.

where $\hat{\mathbf{x}}^W$ is the *estimated location vector* of the SPmap and $\mathbf{p}^W$ is the *perturbation vector* of the SPmap:

$$\hat{\mathbf{x}}^W = \begin{bmatrix} \hat{\mathbf{x}}_{WR} \\ \hat{\mathbf{x}}_{WF_1} \\ \vdots \\ \hat{\mathbf{x}}_{WF_{N_F}} \end{bmatrix} \quad ; \quad \mathbf{p}^W = \begin{bmatrix} \mathbf{d}_R \\ \mathbf{p}_{F_1} \\ \vdots \\ \mathbf{p}_{F_{N_F}} \end{bmatrix} \tag{4}$$

The true location of the robot and the map features is:

$$\mathbf{x}^W = \hat{\mathbf{x}}^W \oplus (\mathbf{B}^W)^T \mathbf{p}^W \tag{5}$$

where the composition operator $\oplus$ applies in this case to each of the components of the vectors, and $\mathbf{B}^W$ is the *binding matrix* of the SPmap, a diagonal matrix formed by the self-binding matrix of the robot and the self-binding matrices of the map features:

$$\mathbf{B}^W = \mathrm{diag}\left(\mathbf{B}_R,\ \mathbf{B}_{F_1},\ \ldots,\ \mathbf{B}_{F_{N_F}}\right) \tag{6}$$

The covariance matrix of the SPmap represents the covariance of the estimation of the robot and the map feature locations, the cross-covariances between the robot and the map features, and finally, the cross-covariances between the map features themselves:

$$\mathbf{C}^W = \begin{pmatrix} \mathbf{C}_R & \mathbf{C}_{RF_1} & \cdots & \mathbf{C}_{RF_{N_F}} \\ \mathbf{C}_{RF_1}^T & \mathbf{C}_{F_1} & \cdots & \mathbf{C}_{F_1F_{N_F}} \\ \vdots & \vdots & \ddots & \vdots \\ \mathbf{C}_{RF_{N_F}}^T & \mathbf{C}_{F_1F_{N_F}}^T & \cdots & \mathbf{C}_{F_{N_F}} \end{pmatrix} \tag{7}$$

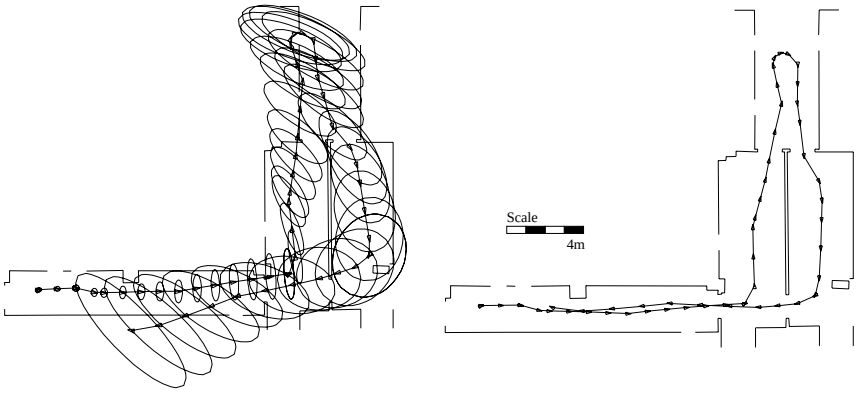

Figure 2. Robot trajectory according to odometry (left) and true trajectory measured with the theodolites (right).

Note that we may represent any type of geometric entity within this general framework. The proposed approach can include different types of features obtained by different types of sensors, and thus it is suitable to deal with a multisensor system. In our experiment, either 2D laser segments or trinocular vertical edges are fused in the estimation of both the robot and the feature locations using an EKF-based algorithm. Figure 1 describes the incremental construction of the SPmap. More details can be found in [7].

3. Experiment Design

3.1. Measurement of the Vehicle Trajectory

The experiment was carried out using a Labmate^{TM} mobile robot, a 2D laser rangefinder and a trinocular vision system, both mounted on the mobile robot, and a pair of theodolites, used as a precise and independent location measurement equipment. At each step of the programmed robot trajectory, the robot location according both to odometry, and measured with the theodolites, were obtained (figure 2). The *environment model* was a set of vertical edges, corresponding to wall corners and door frames, whose location was measured with the theodolites. The location of vertical walls was calculated using this information. This model is used as ground-truth to evaluate the precision of the map building processes. Also at each step of the robot trajectory, the environment was sensed using both sensors as explained below.

3.2. Processing of 2D Laser Readings

A set of 2D points, expressed in polar coordinates with respect to the sensor, were gathered from the surroundings of the vehicle. A maximum range of 6.5 m. and an angular resolution of 0.5 deg. were used during experimentation. Measurement error for each 2D laser reading was modelled by white-gaussian noise mainly characterized by the variances in range and azimuth angle [8]. A two-step segmentation algorithm was applied [9]. First, by application of a tracking-like algorithm, the set of 2D laser readings was divided into groups

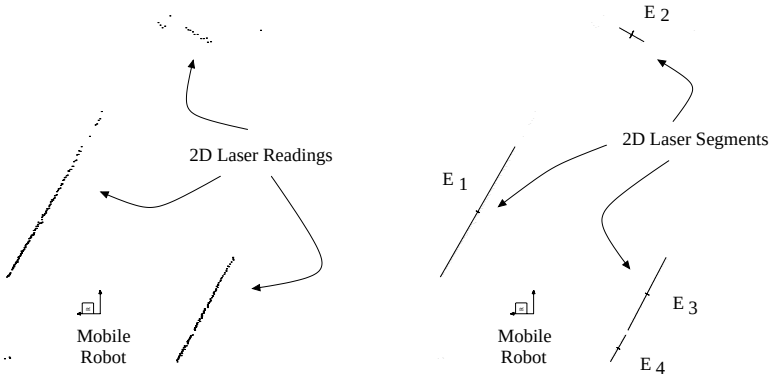

Figure 3. Laser scan and 2D segments obtained at step 38 of the robot trajectory. Lateral uncertainty has been represented for each detected segment.

of points to which a polygonal line without gaps could be fitted. Then, an iterative line fitting technique was considered to detect the endpoints of each 2D segment included in one of those groups. Finally, suboptimal estimation was used to obtain the final representation associated to each laser segment. Also, an estimation of the segment length was computed from the endpoints. Segments shorter than 30 cm. were discarded from further processing. Figure 3 describes an example of segmentation of 2D laser readings gathered during our experimentation.

3.3. Processing of Trinocular Vision

In the case of trinocular vision, large vertical edges were extracted from the three images and matched to obtain the location of trinocular vertical edges corresponding to corners and door frames. The trinocular vision system was composed of three B&W CCD cameras, with a lens focal of $f = 6$ mm., image resolution of 512×512, and camera baselines of 113.7 mm., 110.8 mm. and 186.4 mm. In this work only vertical image segments were considered, allowing deviations from verticallity up to 22.5 deg.

Trinocular stereo processing followed these steps: 1) *image segment detection:* The three images were processed using Burns' algorithm [10]. Three conditions were considered to filter out segments: segments shorter than 100 pixels, non-vertical segments, and segments whose grey-level gradient was smaller than 8 grey levels per pixel; 2) *image segment matching:* using the computed image segments and the calibration information of the cameras (calibration was performed using Tsai's algorithm [11]), images were sequentially processed in a EKF-based predict-match-update loop [12] (matching was performed in 3D to profit from segment overlapping in the image); 3) *image segment projection to 2D:* from the vertical projection of the midpoint projecting ray of each of the matched 3D image segments, the projection ray in 2D was obtained (the standard deviation of the orientation for each projection ray was modelled as 0.1 deg.); 4) *2D vertical edge location:* the 2D location of the vertical segment was computed by fusing the three 2D projection rays. Figure 4 shows the ver-

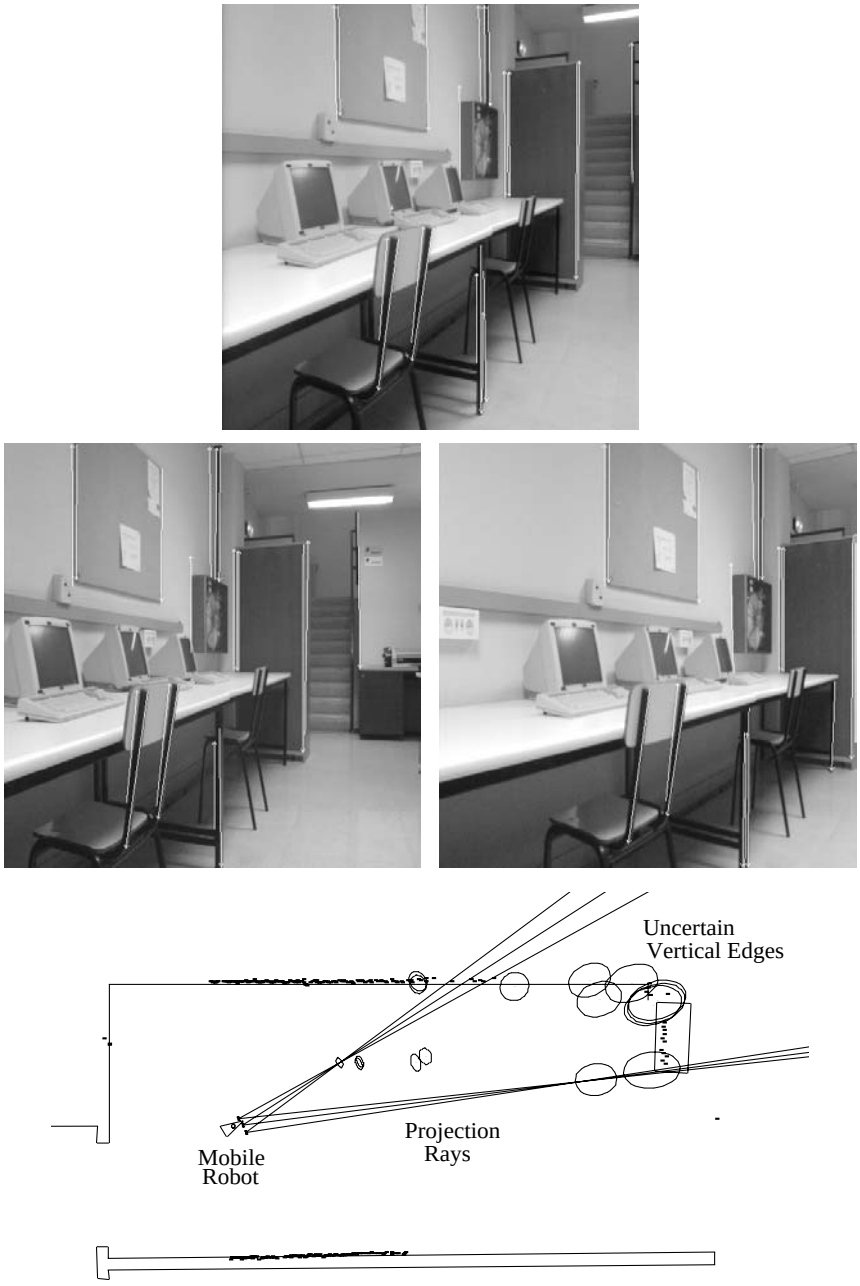

Figure 4. Trinocular image set and vertical edge locations computed at step 38 of the trajectory (only the projection rays for two edges are shown). Elipses show the uncertainty (95% bounds) for the edge absolute location in 2D.

tical edges obtained at step 38 of the robot trajectory, and the 2D local map obtained from the edges matched in the three images.

4. Experimental Results

In the first place, our experiment has shown that the SPmap approach to the simultaneous localization and map building problem is *appropriate* and *general* (figure 5). A statistical test based on the squared Mahalanobis distance was performed to validate the uncertainty model of the robot location for both the 2D laser range finder and the trinocular system solutions. Results showed that the laser-based solution passed the test in more than 95% of the cases, whilst the trinocular-based solution attained 87%. The trinocular-based solution was slightly optimistic due to the fact that the data association problem is more complex and some spurious matchings were accepted. Thus, this approach requires a more ellaborate solution than the closest neighbour used in our experiment. Nevertheless, with both sensors the robot adequately solved the *revisiting problem*, i.e. it recognized previously learned features of the environment.

With respect to *precision*, in our experiments we profited from ground-truth to obtain a precise estimation of the error in the vehicle location computed by each approach. Figure 6 presents the errors obtained at each point of the vehicle trajectory. The laser-based solution was bounded by a 20 cm. error in position and 1.5 deg. in orientation for the location of the vehicle. On the other hand, the trinocular-based approach obtained a maximum error of 35 cm. for the vehicle position and 2.5 deg. in orientation. Thus, the sensorial system based on laser rangefinder increased the accuracy of the solution. The environment map (figure 5) constructed in both cases proved to be adequate for navigation, although the map obtained by the laser-based approach may also be used for path planning purposes, which is not the case for the map obtained with trinocular vision.

The *complexity* of the approach based on trinocular vision is high, because this system requires an ellaborate calibration process, and there is much more computational effort involved. However, laser has been used to its maximum potential. On the contrary, only vertical edges, a minimum potential of the trinocular vision system have been considered. There are many more possibilities with the use of trinocular vision, such as extracting horizontal edges and planar surfaces, to be explored in the future.

5. Conclusions

In this paper we have compared the performance of two distinct sensorial systems on the simultaneous localization and map building problem for a mobile robot navigating indoors: on one hand, a 2D laser range finder, and on the other hand, a trinocular stereo system. The main conclusions derived from our experimentation can be summarized as follows: 1) The simultaneous localization and map building problem, using a non separable state-vector approach is a tractable problem for a reduced number of features. More structured representations are required for large-scale environments; 2) Using a 2D laser range

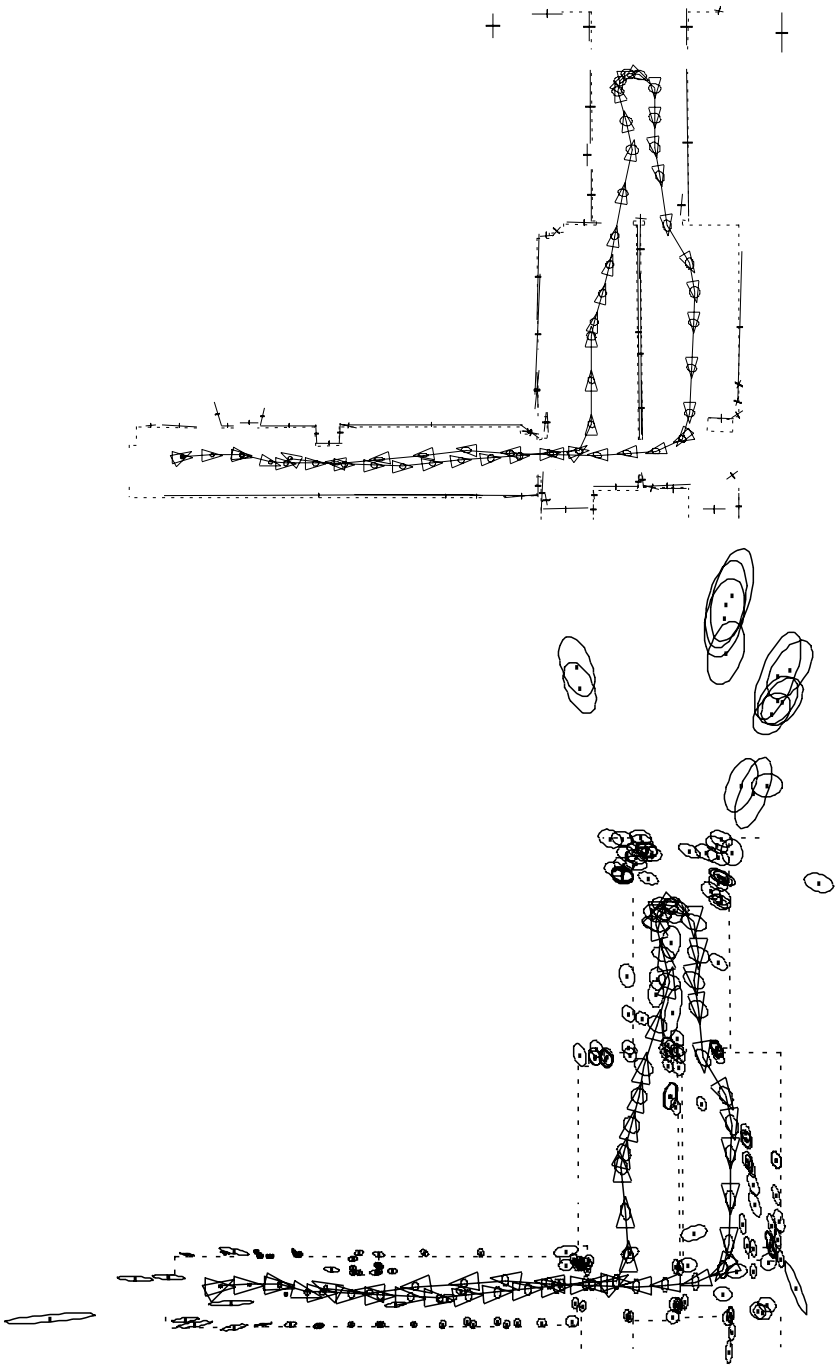

Figure 5. Solutions for the simultaneous localization and map building problem obtained by laser (top) and trinocular (bottom). A hand-measured model map has been drawn for reference purposes.

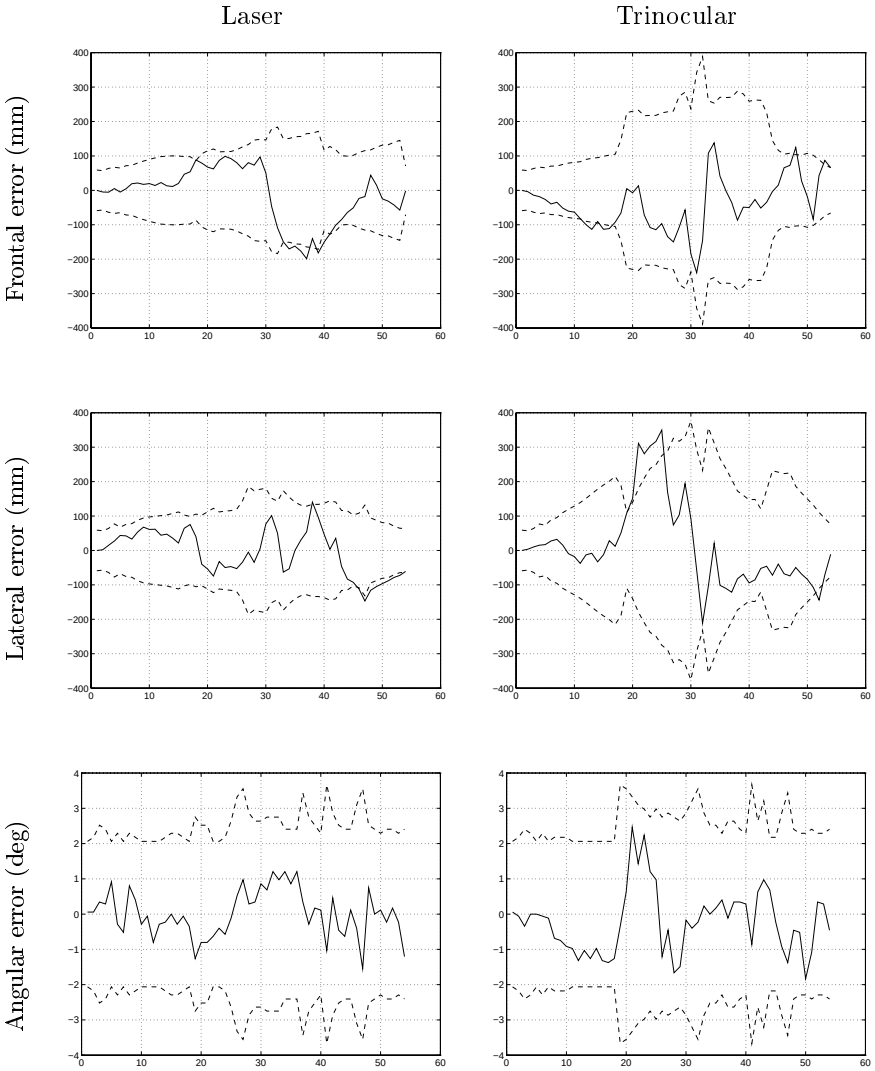

Figure 6. Errors in the robot location estimation and 95% *uncertainty bounds obtained by laser (left) and trinocular (right) along the trajectory of the vehicle.*

finder we obtained a more precise estimated localization for the vehicle than using trinocular vertical edges. One of the reasons was the higher semantical content of laser data as compared with the trinocular data. Also, data association by using the nearest-neighbour technique produced a degradation of the solution obtained by trinocular stereo as compared to the laser-based solution; 3) The laser-based approach allows the structuration of the navigation area towards the topological representation of the environment. However, such an structuration is difficult from the global map obtained by the trinocular-based

approach.

Further work within our group is planned towards increasing the structuration of the navigation area and to profit from multisensor fusion using our general framework for the simultaneous localization and map building problem.

References

[1] R. Smith, M. Self, and P. Cheeseman. Estimating uncertain spatial relationships in robotics. In J.F. Lemmer and L.N. Kanal, editors, *Uncertainty in Artificial Intelligence 2*, pages 435–461. Elsevier Science Pub., 1988.

[2] P. Moutarlier and R. Chatila. Stochastic multisensory data fusion for mobile robot location and environment modeling. In *5th Int. Symposium on Robotics Research*, Tokyo, Japan, 1989.

[3] J.J. Leonard and H.F. Durrant-Whyte. Simultaneous map building and localization for an autonomous mobile robot. In *Proc. 1991 IEEE/RSJ Int. Conf. on Intelligent Robots and Systems*, pages 1442–1447, Osaka, Japan, 1991.

[4] J.D. Tardós. Representing partial and uncertain sensorial information using the theory of symmetries. In *Proc. 1992 IEEE Int. Conf. on Robotics and Automation*, pages 1799–1804, Nice, France, 1992.

[5] J. Neira, J.D. Tardós, J. Horn, and G. Schmidt. Fusing range and intensity images for mobile robot localization. *IEEE Transactions on Robotics and Automation*, 15(1):76–84, 1999.

[6] P. Hébert, S. Betgé-Brezetz, and R. Chatila. Decoupling odometry and exteroceptive perception in building a global world map of a mobile robot: The use of local maps. In *Proc. 1996 IEEE Int. Conf. Robotics and Automation*, pages 757–764, Minneapolis, Minnesota, 1996.

[7] J.A. Castellanos, J.D. Tardós, and G. Schmidt. Building a global map of the environment of a mobile robot: The importance of correlations. In *Proc. 1997 IEEE Int. Conf. on Robotics and Automation*, pages 1053–1059, Albuquerque, NM, U.S.A, April 1997.

[8] J.A. Castellanos. *Mobile Robot Localization and Map Building: A Multisensor Fusion Approach.* PhD thesis, Dpto. de Ingeniería Eléctrica e Informática, University of Zaragoza, Spain, May 1998.

[9] J.A. Castellanos and J.D. Tardós. Laser-based segmentation and localization for a mobile robot. In F. Pin, M. Jamshidi, and P. Dauchez, editors, *Robotics and Manufacturing vol. 6 - Procs. of the 6th Int. Symposium (ISRAM)*, pages 101–108. ASME Press, New York, NY, 1996.

[10] J.B. Burns, A.R. Hanson, and E.M. Riseman. Extracting straight lines. *IEEE Trans. on Pattern Analysis and Machine Intelligence*, 8(4):425–455, 1986.

[11] R.Y. Tsai. A versatile camera calibration technique for high-accuracy 3d machine vision metrology using off-the-self tv cameras and lenses. *IEEE Journal of Robotics and Automation*, 4(3):323–344, 1987.

[12] J.M Martínez, Z. Zhang, and L. Montano. Segment-based structure from an imprecisely located moving camera. In *IEEE Int. Symposium on Computer Vision*, pages 182–187, Florida, November 1995.